NIMROD Applications for MHD Control

Carl Sovinec

University of Wisconsin-Madison

for the

NIMROD Team (https://nimrodteam.org)

16th Workshop on MHD Stability Control

San Diego, CA   Nov. 20-22, 2011

Outline

- Introduction of NIMROD
- Control and control-related applications
  - RF/MHD modeling
  - Disruption mitigation
  - Imposed asymmetry
- Relevant model development
- Concluding remarks

Introduction: NIMROD is a nonlinear macroscopic dynamics code for multi-scale plasma studies.

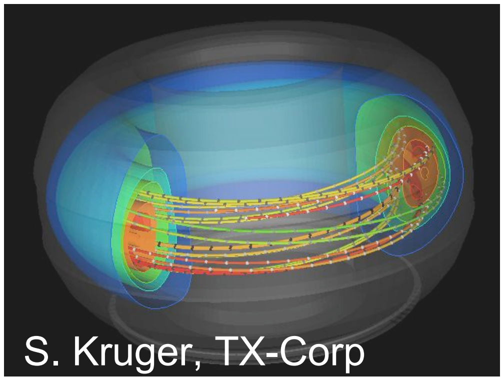

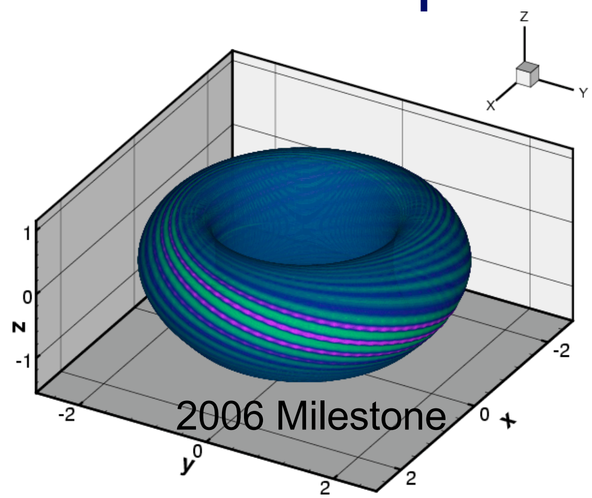

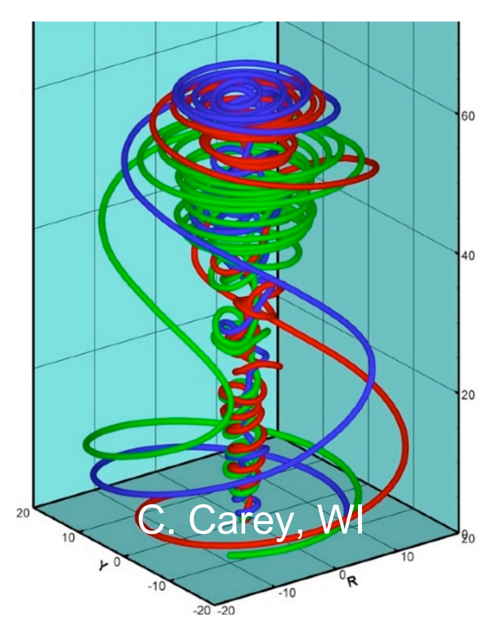

It has been applied to many configurations including:

- Tokamak tearing and ELMS (above)
- MHD jets (above right) and space physics
- Basic plasma phenomena (below right)
- Alternates (below)

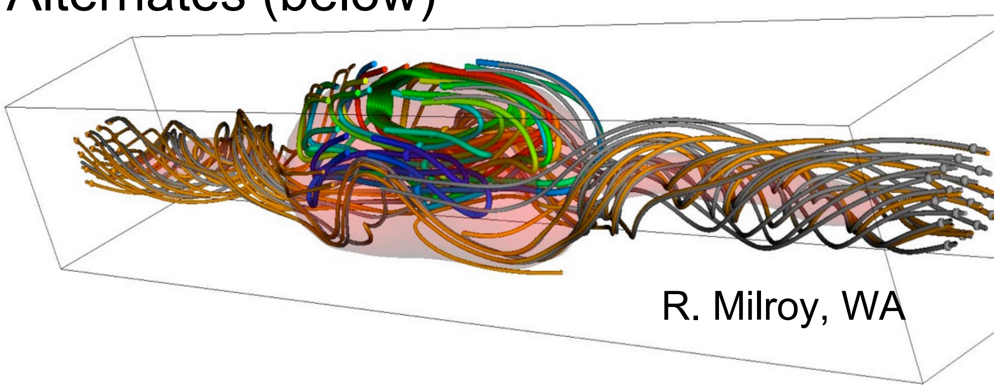

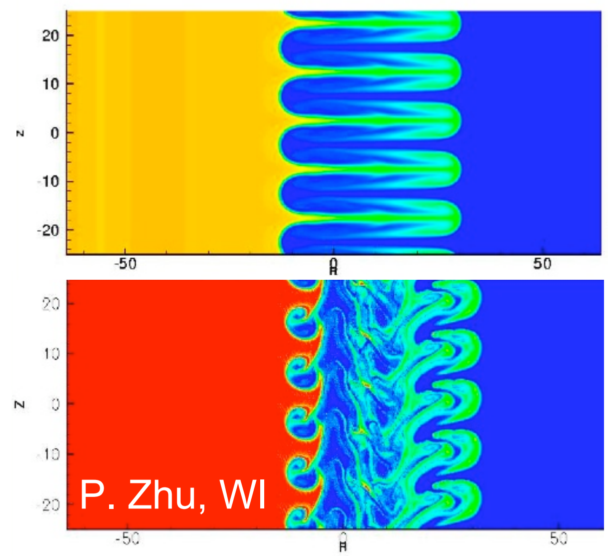

The implementation considers 3D nonlinear dynamics within a geometrically 2D domain.

- The fundamental dependent fields, **V**, **B**, *n*, and *T* (or T_i and T_e), are evolved in time from initial conditions using fluid-based models.

- Variations over the poloidal plane are represented on a mesh of spectral elements.

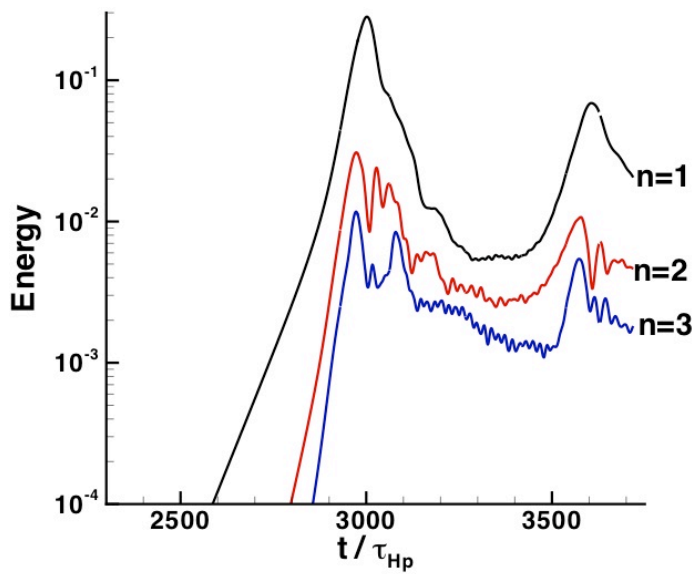

Two-fluid sawtooth evolution of kinetic fluctuation energies. (Comp. has 0≤n≤42.)

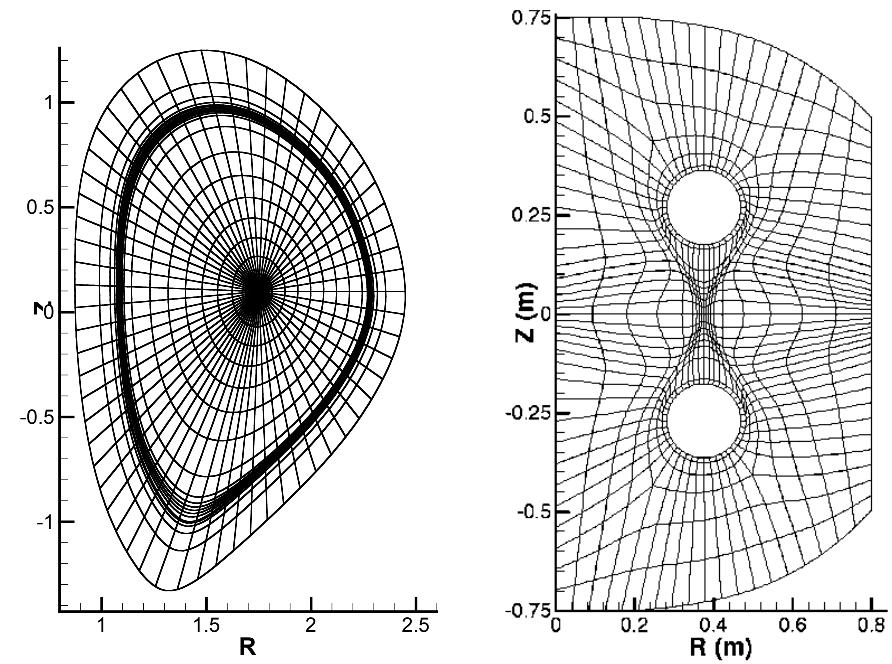

Examples of meshes used for DIII-D tearing (left) and for MRX reconnection (right).

- Variations over the periodic (toroidal or straight) coordinate are represented by finite Fourier series.

Computations related to control include sources or boundary conditions that model the physical system.

• Volumetric sources of momentum density (fluid or electron) and energy density have been used.

• Fluxes and fields applied at the wall may be symmetric or asymmetric.

• A common symmetric flux is the application of E_ϕ from loop voltage.

• An example of asymmetric fields and fluxes are the time-dependent conditions used to model HIT-SI injectors.

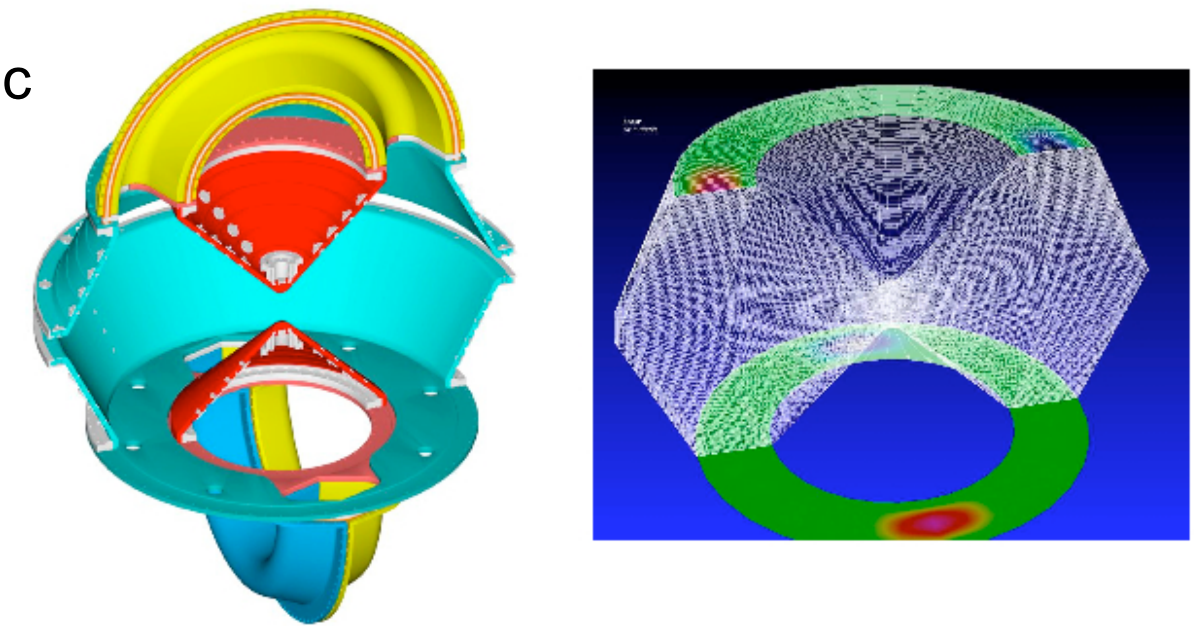

CAD drawing of the HIT-SI spheromak chamber (left) and NIMROD mesh and injector B_z (in color) used in simulation (right). [Izzo and Akcay, Univ. WA]

Control-related applications: To date, the two applications most closely tied to plasma control are RF/MHD coupling and disruption mitigation.

- The RF/MHD effort seeks to model ECCD stabilization of tearing modes as a part of comprehensive simulation capability.
- The project is led by Tom Jenkins of Tech-X in collaboration with Dalton Schnack, Eric Held, and Bob Harvey as part of SWIM.
- Initial work demonstrated island suppression with an ad hoc, toroidally symmetric current drive. [Jenkins, PoP 17, 12502, 2010]

Application of symmetric source affects magnetic islands over the resistive time-scale.

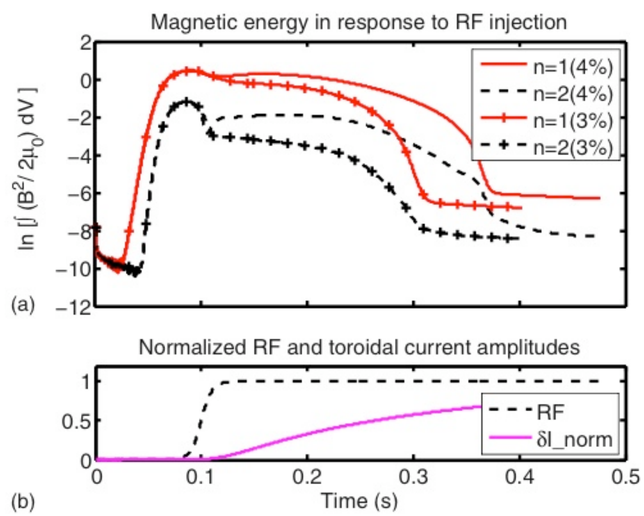

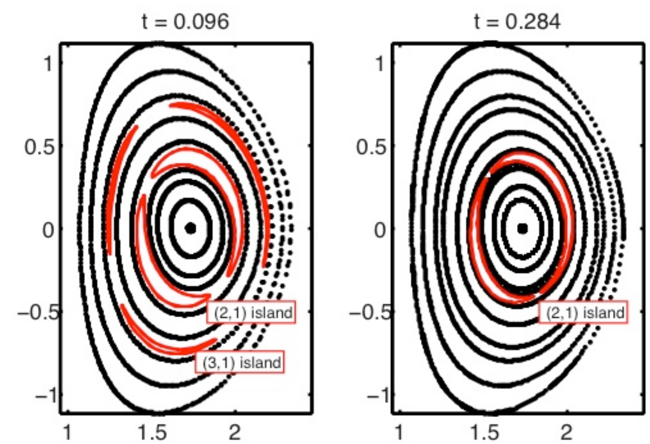

Recent development couples GENRAY ray-tracing and QLCALC diffusion calculation for localized deposition.

- SWIM's Integrated Plasma Simulator (IPS) is used to coordinate computations.
- Present logic is intended to model an ideal system that targets the island O-point.
- Future work will implement more realistic control logic.
- Predicting power requirements for ITER is the primary physics objective.

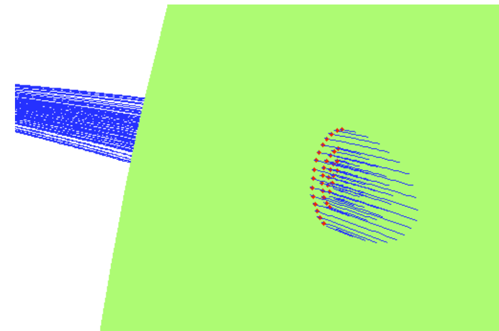

GENRAY ray bundle intercepting NIMROD data plane.

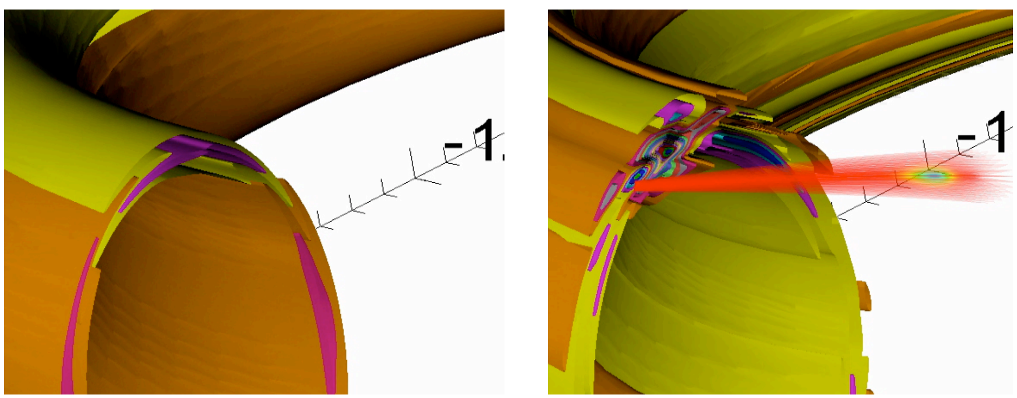

Temperature contours before (left) and just after (right) ECCD feedback on 2/1 island.

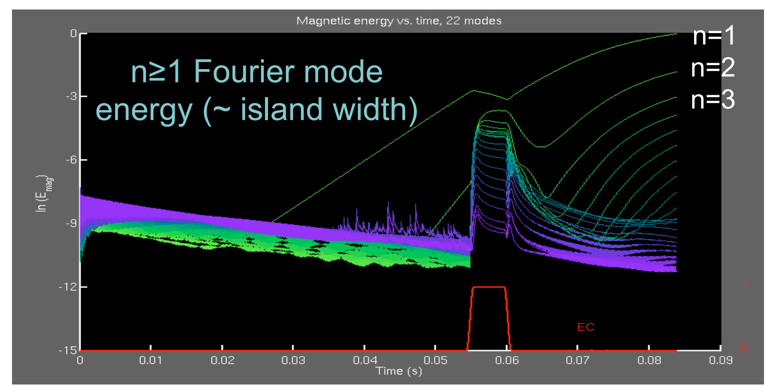

NIMROD magnetic fluctuation energies respond to simulated control.

Disruption mitigation: Simulations of MGI track impurity density and incorporate radiative cooling.

- Val Izzo uses 'NIMRAD' to investigate MHD mixing and resulting efficiency.
- The computations couple NIMROD and the KPRAD radiation code.
- Validation studies have been conducted using T_e and n_e profiles from DIII-D and C-MOD. [Izzo, *et al*., PoP 15, 56109, 2008]

MGI simulation of DIII-D with Ne injection:

1)Injected Ne cools edge, triggers MHD

2)Destruction of flux surfaces reduces Te gradient

3)Core Te drops rapidly due to m=1/n=1 mode

UC San Diego
Local Impact, National Influence, Global Reach

GENERAL ATOMICS AND AFFILIATED COMPANIES

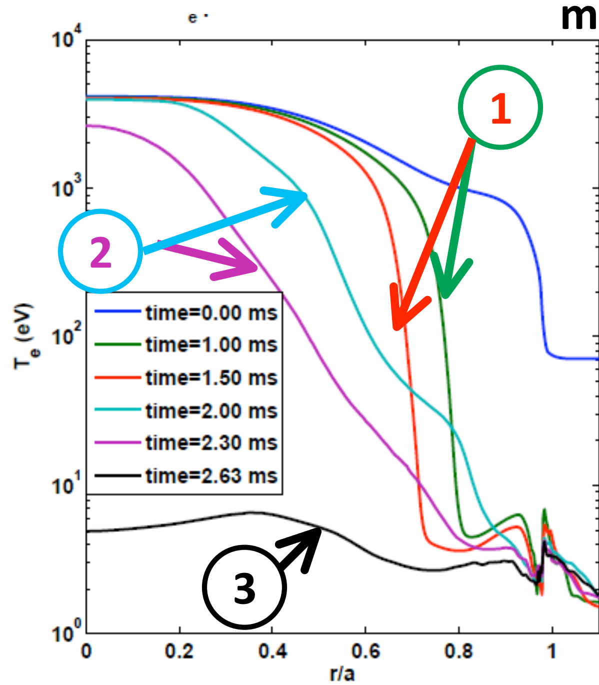

T_e profiles for DIII-D Ne MGI.

Ne density shows efficient mixing into core due to flows associated with 1/1 mode, further enhancing core cooling.

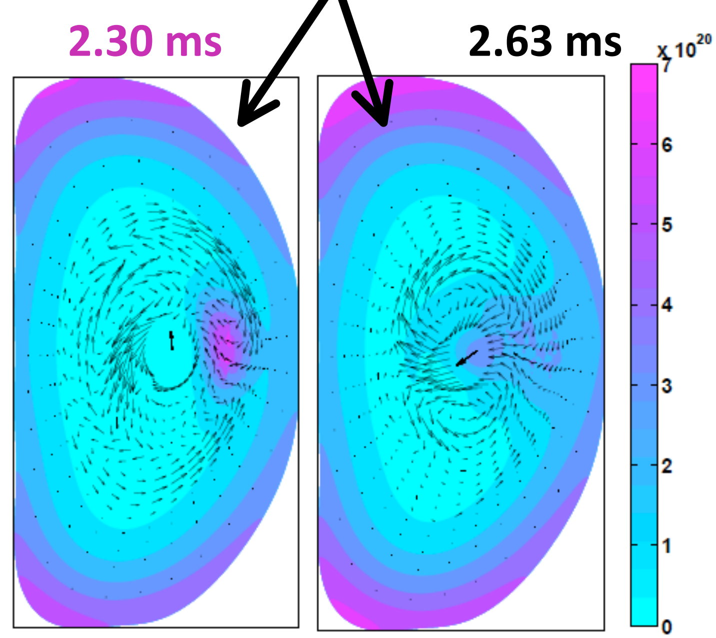

Test-particle model calculates runaway electron (RE) drift orbits as MHD fields evolve.

• Tracer electrons evolved with collisions, ∇B and curvature drifts, bremm-strahlung and synchrotron radiation predict confinement and strike points.

Example RE orbits calculated during NIMROD run; typically thousands per simulation.

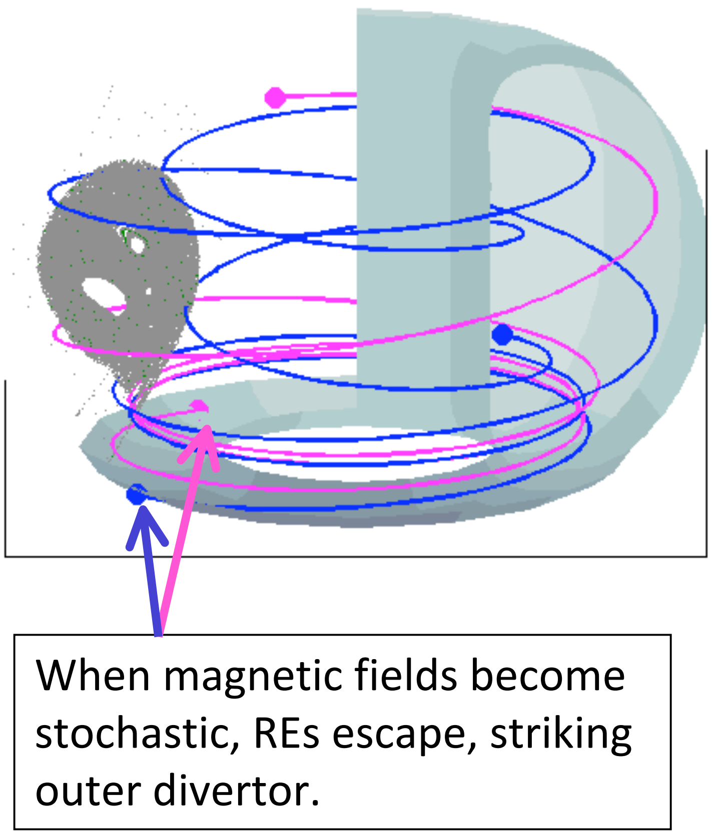

NIMROD predicted RE loss rates show expected relationship to DIII-D measured RE current (with one exception).

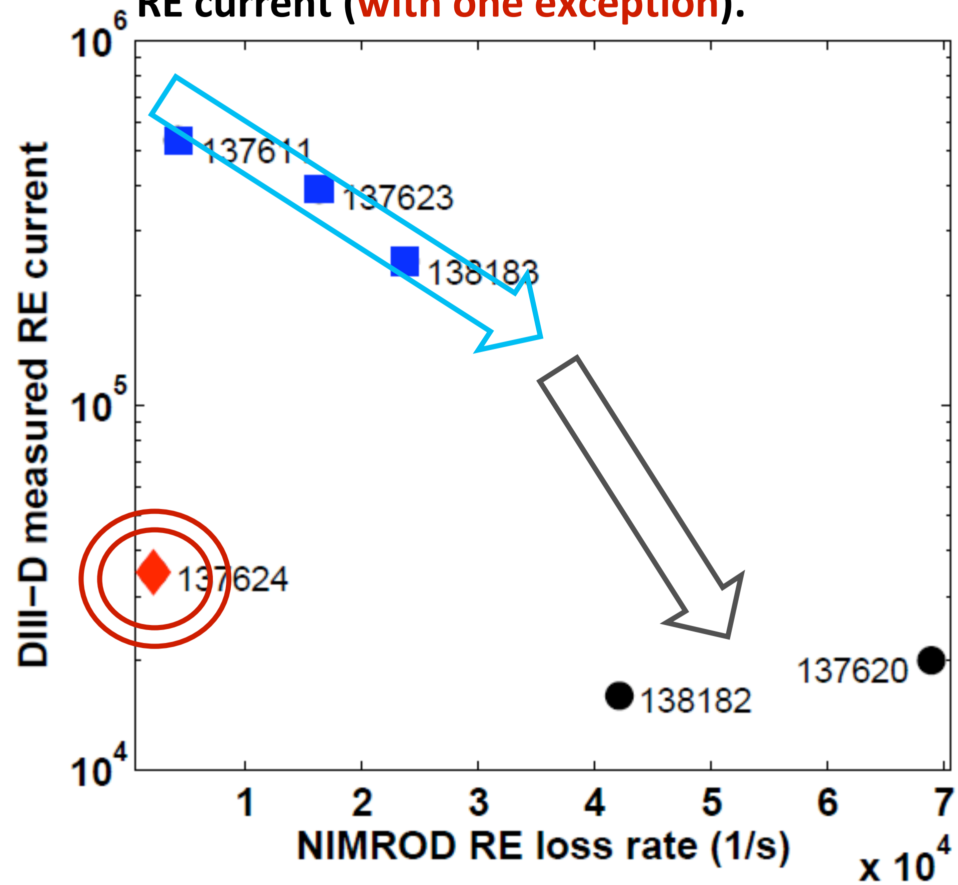

Nonlinear computations with RE tracing and RMP predict little enhancement of losses during thermal quench in DIII-D.

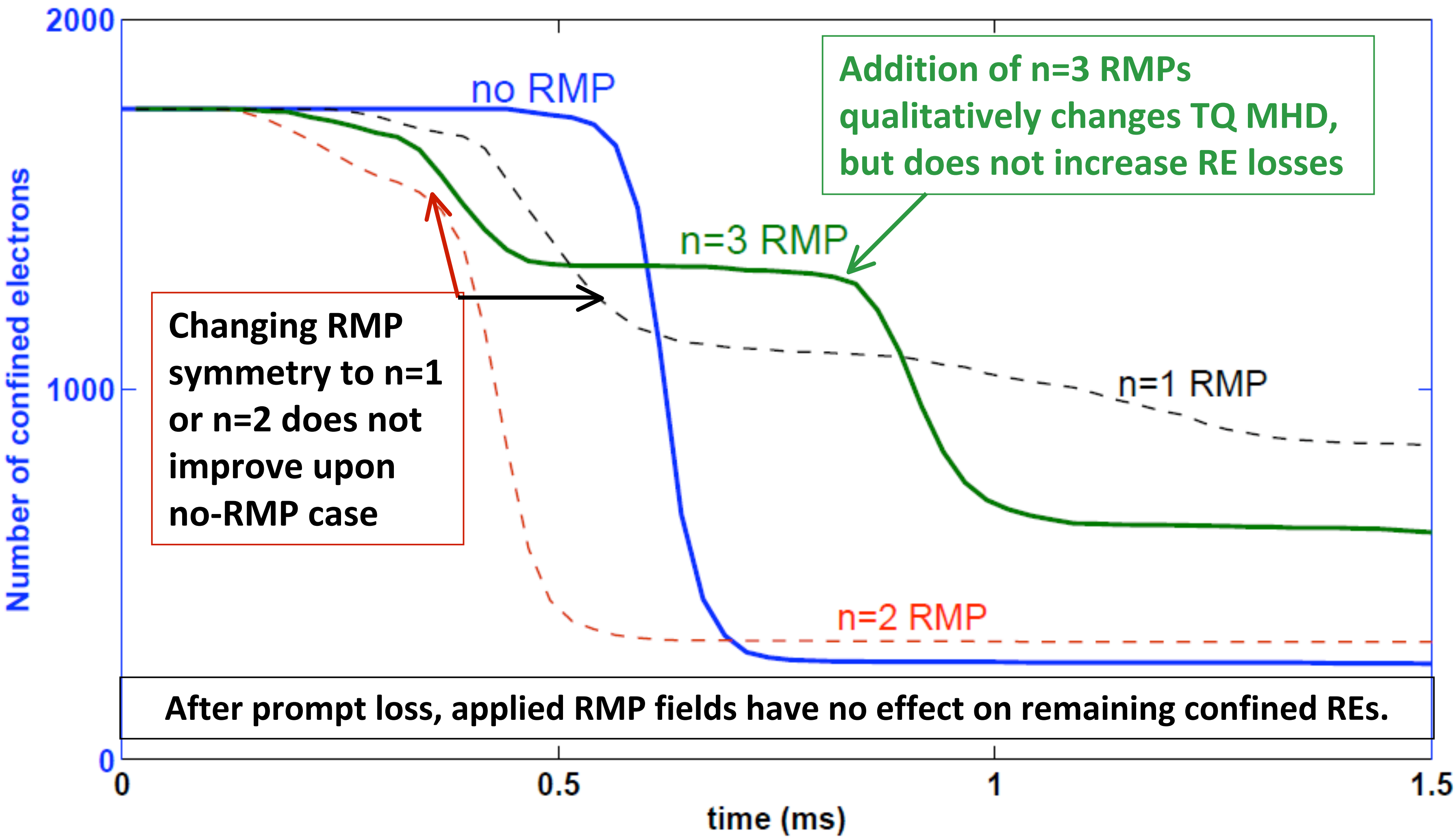

DIII-D experiments showed ambiguous effects of applying n=3 RMPs before TQ, i.e. no clear benefit. As in NIMROD, post-TQ RMPs had no effect.

Imposed asymmetry: Simulations are being used to investigate possible benefits of imposing 3D fields.

- Izzo's DIII-D simulation with n=3 RMP investigates MHD density pump-out.

Plasma response (no rotation)

High edge rotation

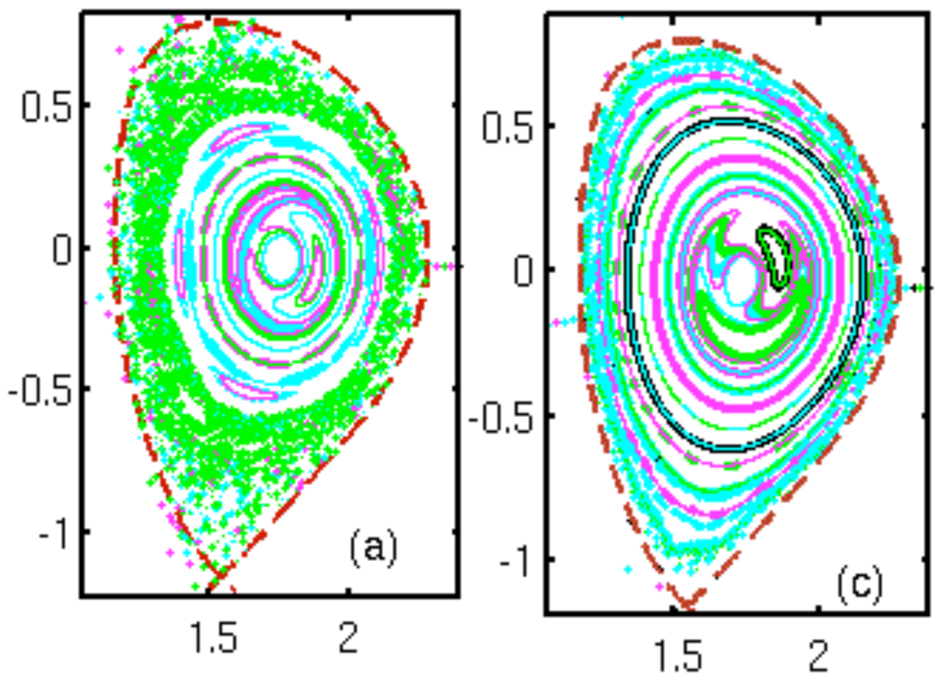

Large toroidal rotation near the edge screens the RMP fields and eliminates the density pump-out effect.

Poloidal Velocity

Density (no rotation)

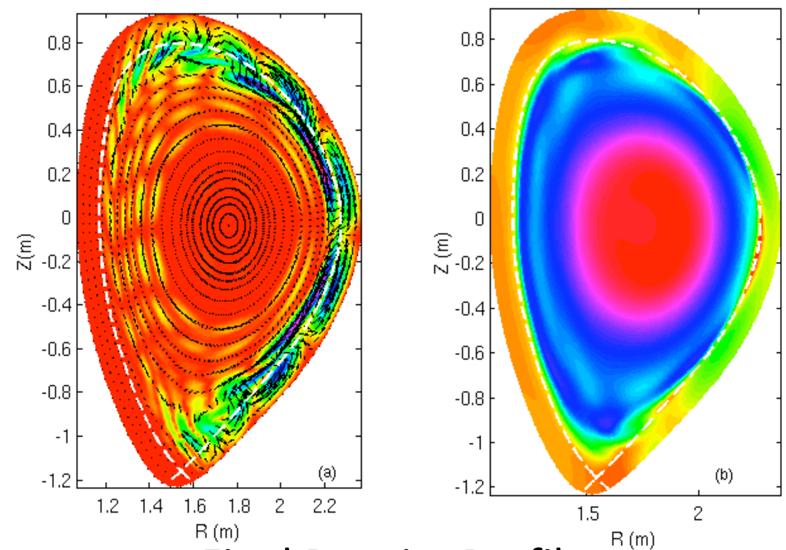

Final Density Profiles

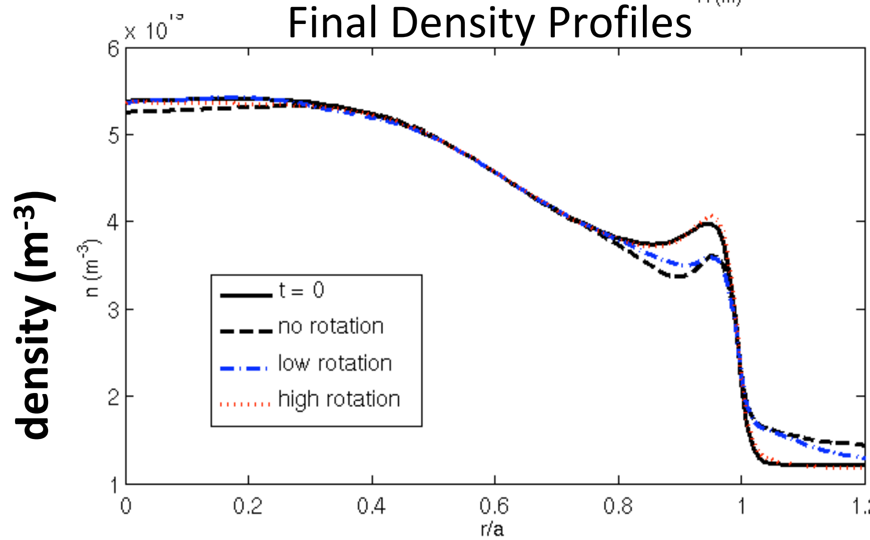

A new RMP study uses circular cross-section toroidal geometry to facilitate analytical comparisons for ELMs.

- Ping Zhu previously performed analytics and computations for an intermediate ballooning regime (no RMP). [Zhu, NF 49, 95009, 2009]
- The new study adds RMP perturbations.

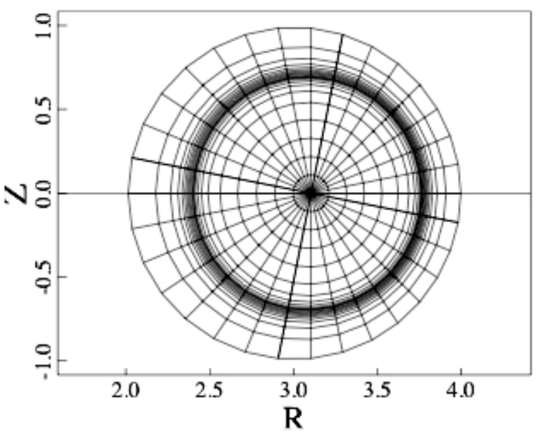

- $\beta \sim 1\%$ at pedestal top
- $n = 7 - 13$ modes weakly unstable

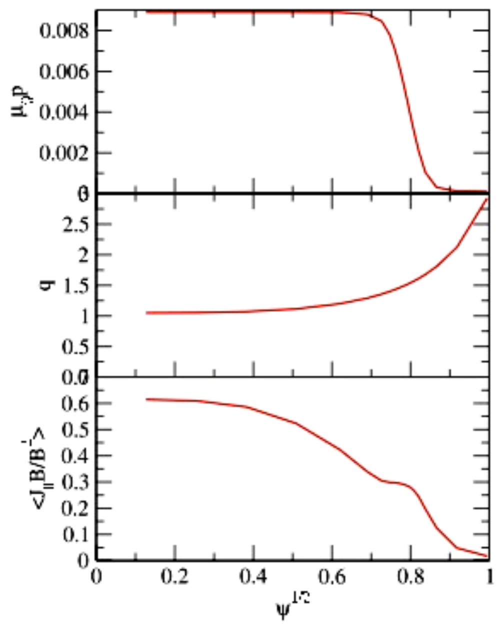

The problem setup has uniform pressure within a pedestal region.

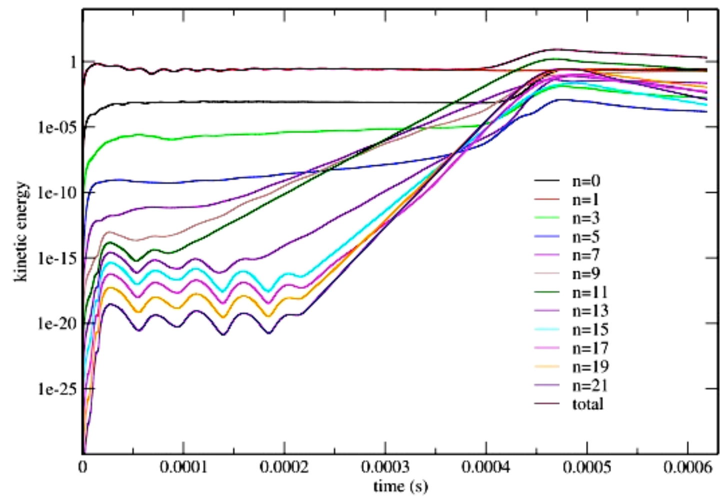

Evolution of perturbed kinetic energy shows RMP effects prior to ballooning saturation.

- **Poincaré surfaces (not shown) have islands before ballooning saturation, a stochastic layer after.**

Computations of the Compact Toroidal Hybrid consider flux-surface evolution with large 3D shaping.

- Auburn's CTH is a heliotron that can have significant rotational transform from plasma current.
- While imposed magnetic fields are asymmetric, helical coils lie outside a toroidally symmetric surface.
- Mark Schlutt (WI) has incorporated vacuum fields provided by Jonathan Hebert (Auburn) into NIMROD boundary conditions.

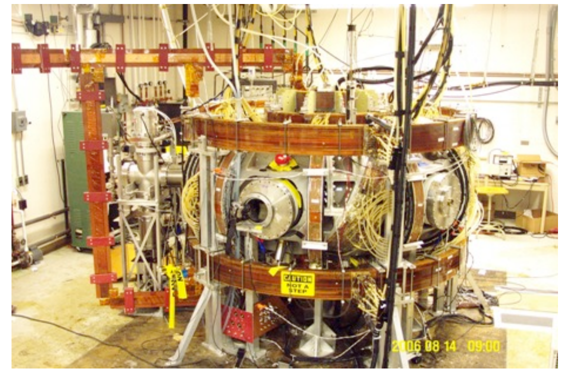

Auburn CTH experiment.

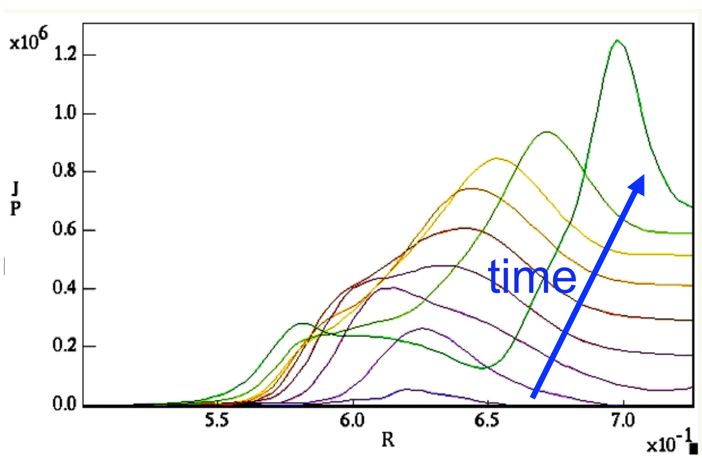

Evolution of J_ϕ profile shows current penetration for applied V_{loop} = 4 V.

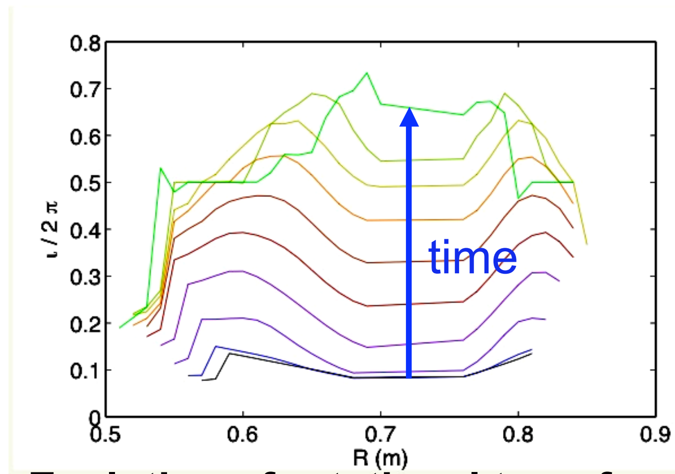

Evolution of rotational transform indicates 2/1 activity late in time.

AUBURN UNIVERSITY

Magnetic topology evolution shows 2/1 island formation prior to loss of flux surfaces.

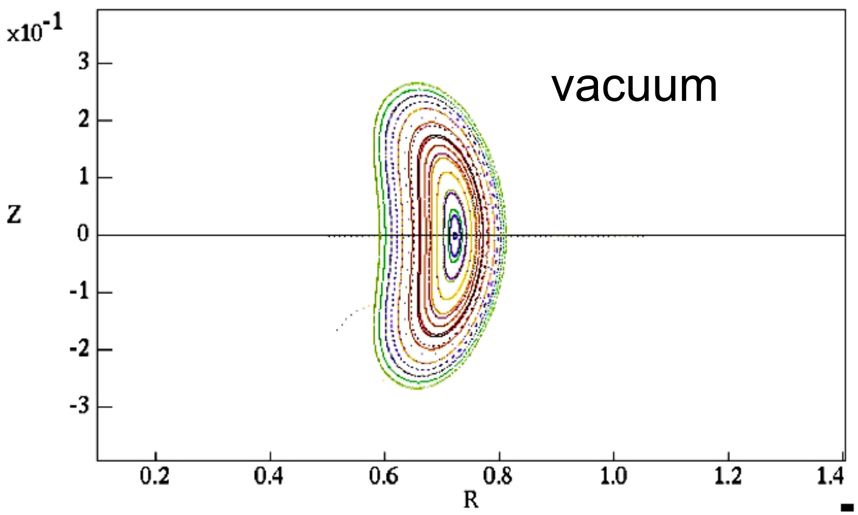

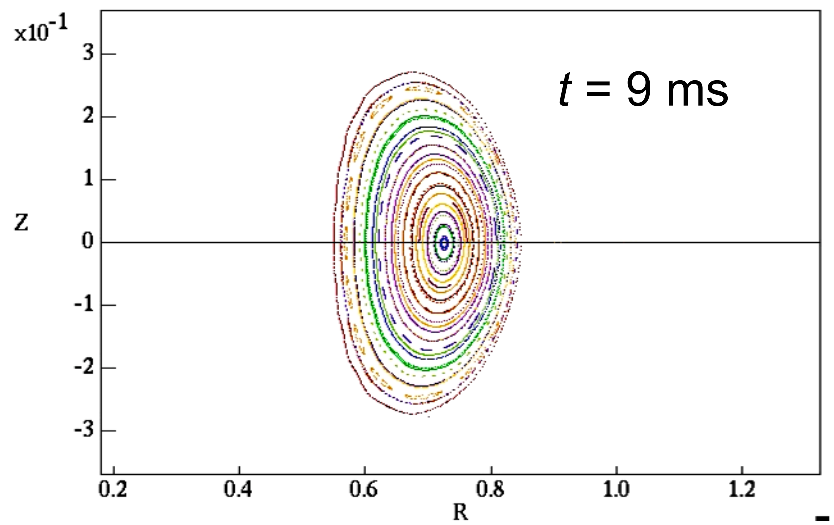

- These 0-β, fixed-resistivity computations show behavior that appears qualitatively similar to the experiment.

- After convergence testing, next steps include temperature evolution to model realistic resistivity profiles that change in time.

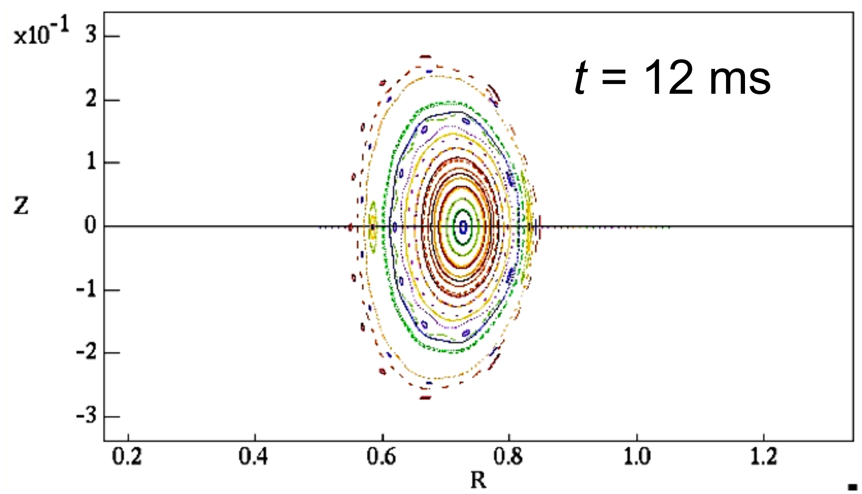

Poincaré surfaces show growth of closed-flux volume then island development.

A study of field-error penetration uses straight cylindrical geometry for verification.

- Andrea Montgomery (WI) has implemented boundary conditions for a thin resistive wall with a helical coil located outside the resistive wall.
- Simple analytical profiles of the form $q(r) = q_0\left[1+(r/a)^{2\lambda}\right]^{1/\lambda}$ are used to select a stable resonant mode.

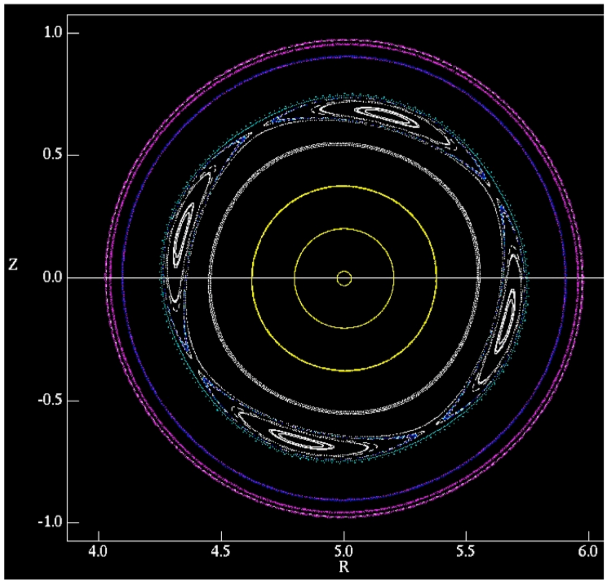

Poincaré surface from a linear computation without flow indicates perturbation amplitude.

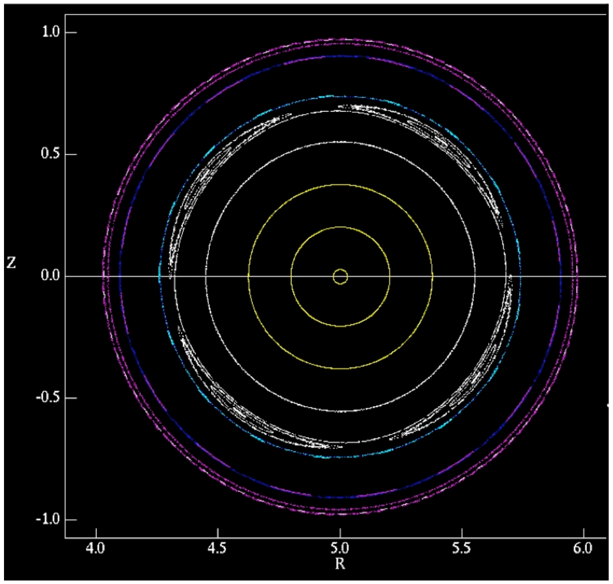

A linear computation with flow shows significant shielding.

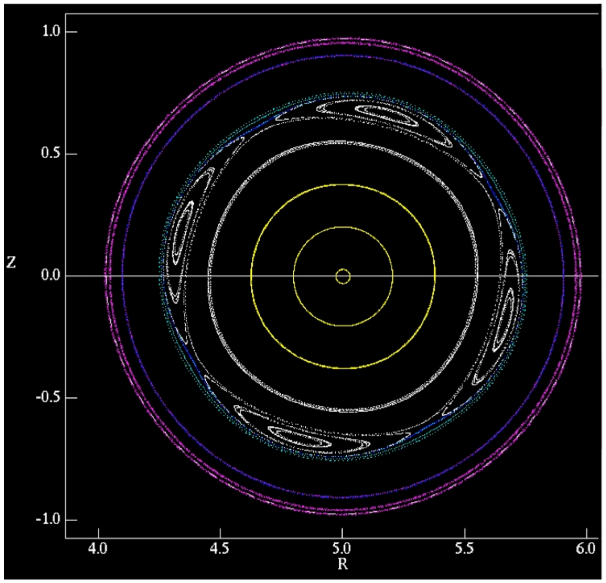

Nonlinear effects with the same flow and perturbation induce locking.

A series of nonlinear computations demonstrates 'sub-critical' locking behavior.

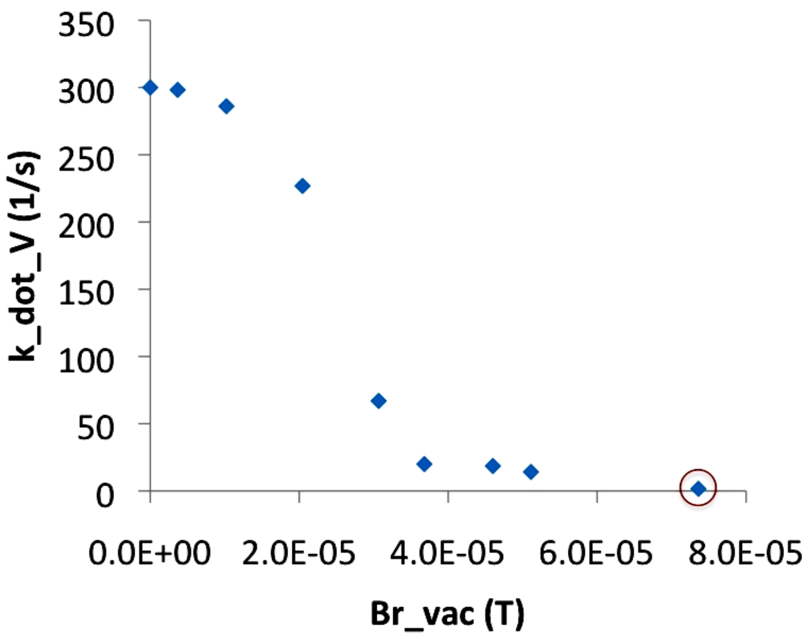

Nonlinear results on k·⟨V⟩ as the perturbation amplitude is varied.

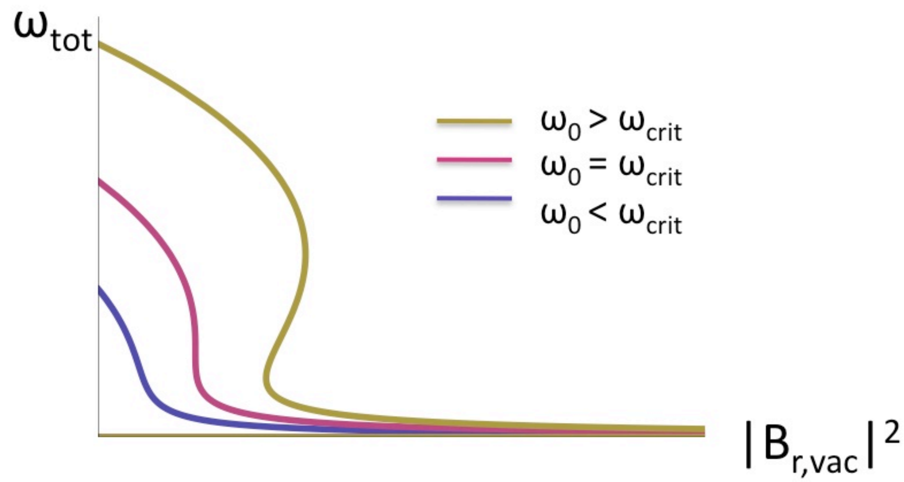

Sketch of different classes of locking behavior for flows that are above and below the critical rate.

- Locking information from Waelbroeck, PFB 1, 1989 and Fitzpatrick PoP 5, 1998 will be adapted for verifying these large-island cylindrical results.
- Computations for less-stable, larger-S (7×10^7) conditions maintain smaller islands and will be used for verifying small-island behavior.
- Testing the response in toroidal geometry is the next computational step.

Relevant model development: Our computations are based on single- and two-fluid plasma models.

$$\frac{\partial n}{\partial t} + \nabla \cdot (n\mathbf{V}) = 0$$ particle continuity

$$mn\left(\frac{\partial}{\partial t} + \mathbf{V} \cdot \nabla\right)\mathbf{V} = \mathbf{J} \times \mathbf{B} - \nabla \sum_{\alpha} nT_{\alpha} - \nabla \cdot \underline{\Pi}$$ flow evolution

$$\frac{3}{2}n\left(\frac{\partial}{\partial t} + \mathbf{V}_{\alpha} \cdot \nabla\right)T_{\alpha} = -nT_{\alpha}\nabla \cdot \mathbf{V}_{\alpha} - \nabla \cdot \mathbf{q}_{\alpha} + Q_{\alpha}$$ temperature evolution

$$\frac{\partial \mathbf{B}}{\partial t} = -\nabla \times \left[\eta \mathbf{J} - \mathbf{V} \times \mathbf{B} + \frac{1}{ne}\mathbf{J} \times \mathbf{B} - \frac{T_e}{ne}\nabla n + \frac{m_e}{ne^2}\frac{\partial}{\partial t}\mathbf{J}\right]$$ Faraday's / Ohm's law

$$\mu_0 \mathbf{J} = \nabla \times \mathbf{B}$$ low-ω Ampere's law

$$\nabla \cdot \mathbf{B} = 0$$ divergence constraint

- Closures for stress ($\underline{\Pi}$) and heat flux ($\mathbf{q}$) often use relations for collisional plasma for practical modeling.

$\underline{\Pi}$ for collisional plasma is a combination of $\underline{\Pi}_{\mathrm{gv}}$, $\underline{\Pi}_{\parallel}$, and $\underline{\Pi}_{\perp}$.

$$\underline{\Pi}_{\mathrm{gv}} = \frac{m_{\mathrm{i}} p_{\mathrm{i}}}{4eB}\left[\hat{\mathbf{b}} \times \underline{\mathbf{W}} \cdot \left(\underline{\mathbf{I}} + 3\hat{\mathbf{b}}\hat{\mathbf{b}}\right) - \left(\underline{\mathbf{I}} + 3\hat{\mathbf{b}}\hat{\mathbf{b}}\right) \cdot \underline{\mathbf{W}} \times \hat{\mathbf{b}}\right], \qquad \left(\underline{\mathbf{W}} \equiv \nabla \mathbf{V} + \nabla \mathbf{V}^{\mathrm{T}} - \frac{2}{3}\underline{\mathbf{I}}\nabla \cdot \mathbf{V}\right)$$

$$\underline{\Pi}_{\parallel} = \frac{p_i \tau_i}{2}\left(\hat{\mathbf{b}} \cdot \underline{\mathbf{W}} \cdot \hat{\mathbf{b}}\right)\left(\underline{\mathbf{I}} - 3\hat{\mathbf{b}}\hat{\mathbf{b}}\right)$$

$\underline{\Pi}_{\perp} \sim -\dfrac{3 p_i m_i^2}{10 e^2 B^2 \tau_i}\underline{\mathbf{W}}$ has been treated as $-nm_i \nu_{iso}\underline{\mathbf{W}}$ or $-nm_i \nu_{kin}\nabla\mathbf{V}$

Kinetic modeling of energetic ions is available, and majority-species drift kinetics is under development.

- Charlson Kim (WA) implemented and verified PIC-based δf computation for minority energetic particles; drift and full-Lorentz options are available.
- A relatively recent application is Dylan Brennan's (U-Tulsa) study of energetic-ion effects on 2/1 tearing in large tokamaks.
- Eric Held is developing drift-kinetic modeling with a complete linearized Coulomb collision operator for neoclassical effects in 3D evolution.
- Comparison of bootstrap current over a NIMROD 2D spatial domain with results from E. Belli's 1-spatial-D NEO code provides an important verification.
- Full RF/MHD coupling will incorporate DK modeling a la Hegna&Callen, PoP 16, 112501, 2009.

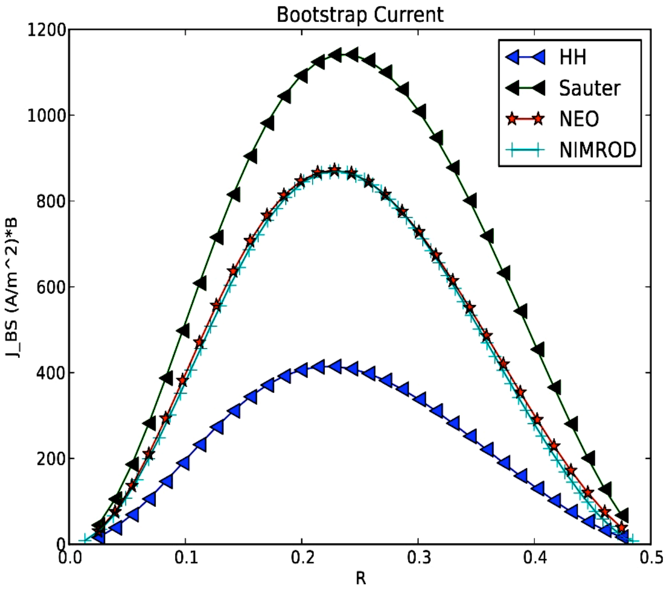

Comparisons of NEO's flux-surface averaged bootstrap current with results from NIMROD's DKE solution.

Concluding Remarks

• Many current NIMROD modeling applications are related to plasma control, either directly or indirectly.

• The applications include boundary conditions or sources that model how external controls influence magnetized plasma over long time-scales.

• Many NIMROD applications are conducted by university faculty, staff, and students.

• To benefit all applications, significant active development of NIMROD continues after more than 15 years.

Rough outline of control system logic

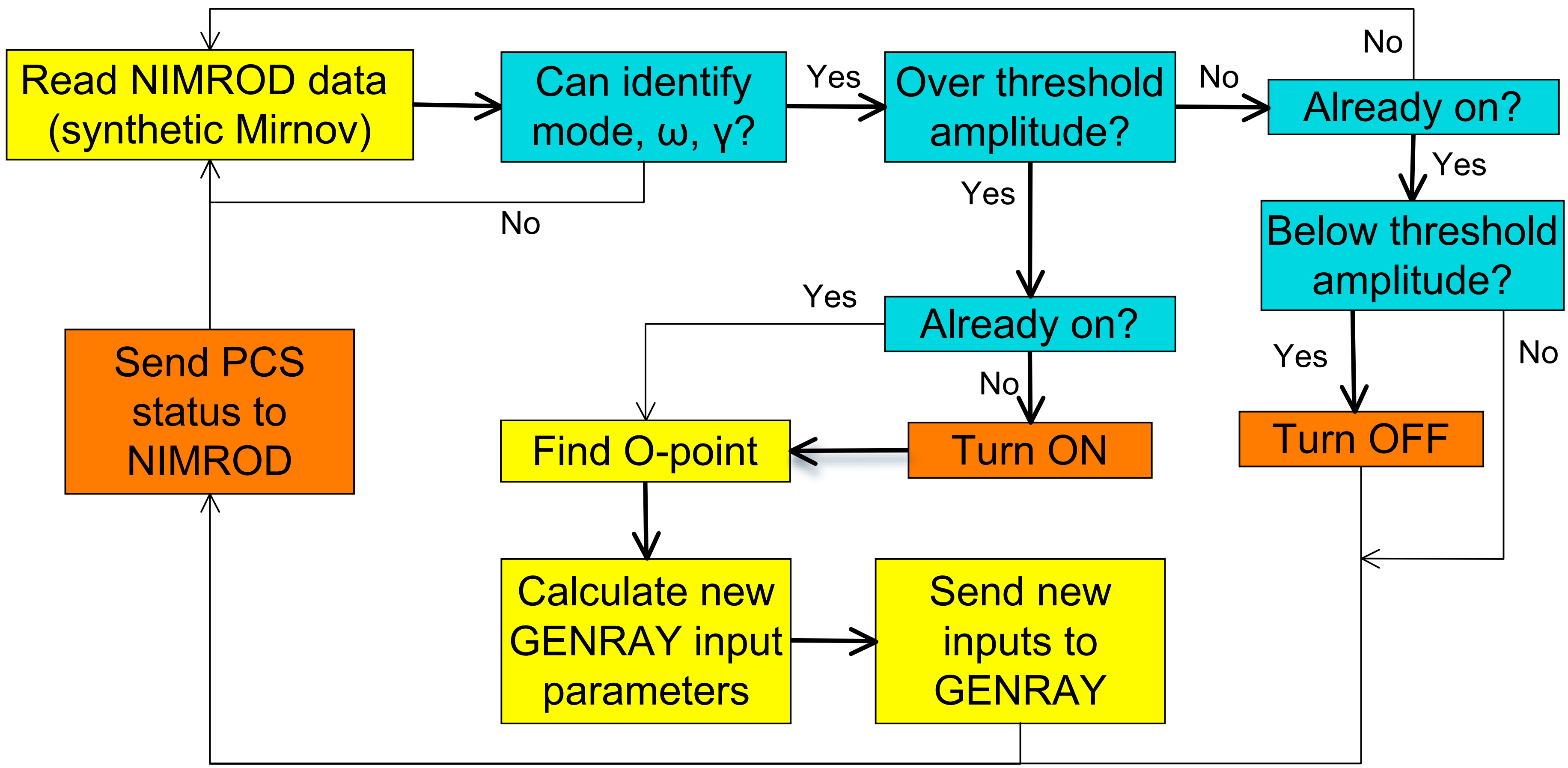

Hierarchy of control systems desired:

- "Dumb system": Mirnov coils only (for detection)
- Experimental mimicking system: Implement system similar to DIII-D
- Optimized control system: What we want to provide
- "Perfect system": Hit the O-point exactly (what we are doing in this talk)